



ORIGINAL PAPER

R. R. Mulyukov · G. F. Korznikova · K. S. Nazarov ·
R. Kh. Khisamov · S. N. Sergeev · R. U. Shayachmetov ·
G. R. Khalikova · E. A. Korznikova

Annealing-induced phase transformations and hardness evolution in Al–Cu–Al composites obtained by high-pressure torsion

Received: 4 June 2020 / Revised: 20 September 2020 / Accepted: 15 October 2020 / Published online: 10 January 2021
© Springer-Verlag GmbH Austria, part of Springer Nature 2021

Abstract Multilayered bulk Al–Cu–Al metal-matrix composite was fabricated by means of high-pressure torsion and subsequent annealing. The resulting composite had a heterogeneous structure consisting of ductile aluminum matrix and hard intermetallic inclusions with a gradient decrease in grain size and layer thickness when moving from the center to the periphery of the sample. Precipitation of Al₂Cu intermetallic phase was revealed at the edge of the sample in the as-deformed state. Post-deformation annealing initiated the emergence of AlCu and Al₄Cu₉ intermetallic precipitates with increased hardness compared to strain-induced Al₂Cu particles. The growth kinetics of intermetallic compounds was obtained using precise X-ray phase analysis. It was found that the initial growth of intermetallic phases at temperatures 150–210 °C depends on time $t^{1/2}$, indicating the bulk diffusion-controlled growth. The growth activation energy of Al₂Cu and AlCu phases was calculated to be 0.48 and 0.33 eV, respectively. The results obtained contribute to an understanding of the kinetics of annealing-induced growth of intermetallic phases and the corresponding evolution of strength characteristics in Al–Cu–Al composites. It was revealed that thermal treatment regimes resulting in enhanced mechanical properties are associated with moderate time and temperature of annealing, which allows avoiding partial dissolution of strengthening phases. The applied approach of phase kinetics analysis can become the basis for the development of new energy-efficient heat treatment modes of in situ Al-based composites allowing to govern their heterogeneity type and tailoring the mechanical properties of the material.

1 Introduction

In recent years, the attention of many researchers has been attracted to aluminum-based metal matrix composites (MMC), due to their high specific strength, hardness, wear resistance and fatigue strength [1–5]. One can distinguish two types of composites. Namely, those that are ex situ composites, where the reinforcing particles are incorporated into the matrix, and in situ composites, where hardening is realized via phase transition-induced emergence of precipitates [6,7]. Both approaches allow obtaining composites with unusual combinations of strength-to-weight ratio stiffness, high-temperature performance and hardness.

Composites fabricated by the ex situ method suffer from limitations originating from the weak bond between the particles and the matrix and inhomogeneous distribution of reinforcing particles [4,8], meanwhile having

R. R. Mulyukov · G. F. Korznikova (✉) · K. S. Nazarov · R. Kh. Khisamov · S. N. Sergeev · R. U. Shayachmetov ·
G. R. Khalikova · E. A. Korznikova
Institute for Metals Superplasticity Problems of the Russian Academy of Sciences, 39 Khalturin Street, Ufa, Russia 450001
E-mail: gfkornikova@gmail.com

R. R. Mulyukov
Ufa State Petroleum Technological University, 1 Kosmonavtov Street, Ufa, Russia 450064

E. A. Korznikova
Ufa State Aviation Technical University, 12 Karl Marx Street, Ufa, Russia 450000

low cost and manufacturing simplicity [9] that provides a wide range of applications for these materials [7, 10, 11]. In situ MMC are more exigent in terms of technology and production expenses nevertheless being in high demand due to several advantages such as thermodynamical stability, strong interfacial bonding and uniform reinforcing particles distribution [8]. A wide range of approaches of MMC production are being developed due to their high relevance in frames of potential applications. Among existing MMC synthesis techniques, one can recall powder metallurgy [12], stir casting [13], reactive slag process [14], squeeze casting [15], spray deposition techniques [16], flux assisted synthesis [17], cold rolling [18] and diffusion bonding [2]. However, processing features of composites are not always well established, and associated physical mechanisms are not deeply understood [6]. Filling this gap is a prerequisite for improving the performance of in situ MMC in frames of commercial applications.

Numerous investigations of Al-based in situ composites have been performed up to date addressing features of their synthesis and operation performance [9–12, 14–16, 18]. It is widely recognized that the properties of MMCs are controlled by the size, morphology and volume fraction of the reinforcements as well as the nature of the matrix–reinforcement interfaces. Severe plastic deformation was found to be an effective tool for managing the above-mentioned parameters. This method has been successfully used for formation of homogeneous composite structures in Al–Mg [2, 19], Al–Cu [20], Al–Ti [21], Zn–Mg [22] Cu–steel [23], bronze–Nb [24], Cu–graphene [25] and many other systems [3]. Among all considered systems, the Al–Cu combination is the most ductile one due to high symmetry fcc lattice of both components meanwhile having several intermetallic compounds on the mutual solubility diagram [26] that allows to reach high values of both ductility and hardness by appropriate choice of thermo-mechanical treatment. The possibility of structure management is of particular importance because the maximum use temperature of the composite is defined by the temperature of the strengthening precipitates coarsening.

High-pressure torsion (HPT) is a method associated with a high energy impact on the material where part of the strain energy can be dissipated via nonequilibrium phase transition emergence [27, 28]. This feature was successfully used for the synthesis of Cu–Al [20] bulk composites with extreme hardness at the disk peripheries and with low hardness at the disk centers. Increase in hardness can be explained by the HPT-induced promotion of the solid-state reaction [29] in constrained metals where the mutual dissolution of Al and Cu is accompanied by the formation of Al_2Cu , AlCu and Al_4Cu_9 intermetallic phases [3]. One should keep in mind that final mechanical properties of the MMC are defined by the chemical composition and distribution of intermetallic precipitates which in turn is the result of enhanced strain-induced diffusion due to the presence of numerous lattice defects. Among possible ways to increase the homogeneity of the MMC, one can recall post-deformational thermal treatment associated with phase composition evolution.

Establishing thermal treatment regimes allowing to reach some definite level of mechanical properties is not possible without knowledge of the kinetics of phase transformations in the studied systems in nonequilibrium conditions. This feature has been poorly addressed in the literature [3, 29]. Thus, it was shown that estimated diffusion coefficients during HPT are 10^{12} – 10^{22} times higher than for conventional lattice diffusion and are comparable to surface diffusion [3]. In [30], the activation energy of intermetallic phases was analyzed, however, without any correlation with mechanical properties evolution during the phase composition change. Apparently, this factor can be of particular importance for revealing the parameters defining the strength of the material.

In order to establish the connection between the kinetics of intermetallic phase growth and evolution of mechanical properties, we have performed a pioneering detailed investigation of phase composition evolution upon annealing and analyzed the correlation of the latter with mechanical properties of Al–Cu–Al hybrid composite. The proposed approach—the detailed analysis of contribution of intermetallic phases to the total strength of the material—allows to provide new fundamental insights for possible ways of structure optimization.

2 Experimental details

The experiments for synthesis of Al–Cu composite was performed using conventional metal rods of 99.3–99.5 wt% purity Al and 99.90 wt% purity Cu. The initial rods were subjected to preliminary annealing at 400 and 900 °C for Al and Cu, respectively. The annealed rods had a diameter of 12 mm and were sliced to 0.25 mm thickness discs. Mechanical bonding was performed using a constrained high-pressure torsion machine [27]. Three disks in material sequence Al–Cu–Al (see Fig. 1a) were placed together in a circular groove of the lower HPT anvil. MMC samples were obtained by shear deformation under pressure on Bridgman anvils

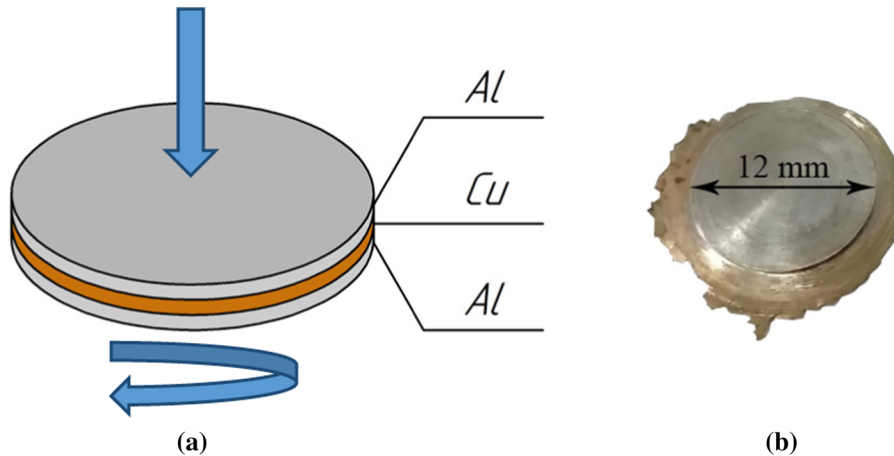


Fig. 1 Scheme of stacking Al and Cu layers (a) and general view of the Al–Cu–Al composite sample obtained by constrained high-pressure torsion (b)

with 12 mm diameter and 0.25 mm depth grooves, at a pressure of 5 GPa, 10 revolutions and a speed of 1 revolution per minute at room temperature. Preliminary experiments revealed that solely compression impact not accompanied by torsion does not lead to the bonding of contacting layers and shear deformation is required for bulk composite formation. The minimum number of revolutions required to obtain the bulk in situ composite at the pressure of 5 GPa was found to be 10. The typical appearance of the composite samples obtained in the above described conditions in the as-processed state is shown in Fig. 1b.

Samples were isothermally annealed at temperatures of 150, 170, 190 and 210 °C in a time interval from 1 to 120 min. The annealing time intervals were a subject of subsequent increase in order to follow the nonlinear kinetics of intermetallic phase growth.

The kinetics of phase transformations in the obtained composite was studied on the entire surface of the cross section of the sample by means of the X-ray phase method using Cu- $K\alpha$ radiation. For accurate quantitative phase analysis, the diffraction patterns were recorded on a Rigaku Ultima IV using a narrow parallel high-intensity X-ray beam, and the volume fraction of phase precipitates was calculated using the Rietveld method, which made it possible to determine the phase fraction with an accuracy of not worse than 0.2%. The microstructure after microhardness measurements was studied on a Carl Zeiss ISM-5 laser scanning microscope in optical mode.

To analyze the microstructure and phase composition after HPT and annealing, a scanning electron microscope (SEM) TESCAN VEGA 3SBH equipped with energy-dispersive spectrometry (EDS) was used. Microstructure investigations were performed by means of a phase contrast-based backscattering electron detector for local phase identification. The energy-dispersive analysis was conducted along the sample thickness and radius in order to estimate the overall degree of uniformity.

Transmission electron microscopy (TEM) studies were performed on a JEM 2100 Plus microscope at accelerating voltage of 200 kV. The electron diffraction pattern was taken from a area of $2 \mu\text{m}^2$.

Microhardness was measured by an Vickers method on an AFFRI DM8A microhardness tester with an indentation load of 10 g.

3 Results and discussion

3.1 Microstructure in as-deformed state

As was shown previously in [20] by means of an SEM analysis of the cross section of the deformed Al–Cu–Al composite, the sample has bulk porousless structure with inhomogeneous component mixture along the sample radius. White region on the micrographs represents a Cu-rich phase, and the gray region represents the Al-based phase (Fig. 2). In the central part highlighted with a square 1, the sample has three layers. A more uniform cross-sectional structure is observed in the area near the middle of the radius highlighted with a square 2 (Fig. 2c), and the highest mixing degree accompanied by formation of nanolaminated structure is observed in the vicinity of the sample edge, where the thickness of the nanolayers does not exceed 100 nm (Fig. 2d). In

general, this gradient of mixing degree corresponds well to the strain distribution in sample after HPT which grows monotonically upon the radius increase [27]. This is obviously due to the fact that nonequilibrium mechanical alloying is an effective channel of strain-induced energy dissipation whose effectiveness should increase with deformation degree growth.

Energy-dispersive analysis allows to quantify the mixing degree of the components in different sections of the composite sample. The contrast of the images and the components distribution curves reveal the presence of solely Al and Cu without any intermetallic phases (Figs. 3a–c).

A detailed study of the composite structure in as-deformed state at high magnifications was carried out by means of TEM. An ultrafine-grained single-phase structure with equiaxed defect-free grains of about 0.8 μm in size was revealed in the Al layers at mid-radius (Fig. 3a). The grain boundaries in the Al phase are straight and have relaxed structure and banded contrast, which indicates that dynamic recrystallization occurred in the aluminum component of the composite during HPT. No precipitations were observed in the mid-radius area. Near the disc edge in the areas of the active mixing of the components (Fig. 3b), individual nanoscale nucleation of the Al₂Cu intermetallic phase appears in the nanolayer structure, which is clearly distinguishable in the cross section (Fig. 2). Due to the small grain size, the electron diffraction pattern (SAED pattern) has an almost circular appearance. On the electron diffraction pattern, along with reflections from Al and Cu, reflections with large interplanar spacings corresponding to the Al₂Cu phase are visible.

3.2 Phase transformations upon annealing

Annealing treatment was performed in order to obtain composites with inclusions of additional intermetallic phases. The Al–Cu phase diagram is characterized by many intermetallic phases with complex mutual relationships occurring in all regions of the phase diagram [26]. Thus, several intermetallic phases may appear in the temperature range below 500 °C: Al₂Cu (θ), AlCu (η 2), Al₃Cu₄ (ζ 2), Al₂Cu₃ (δ) and Al₄Cu₉ (γ 1). The most common phases are Al₂Cu, AlCu, and Al₄Cu₉. It also follows from the Al–Cu binary phase diagram that a very small proportion of Cu can be dissolved in Al, while 18% of Al can be dissolved in Cu, i.e., phase transformations in the system are ensured mainly due to the diffusion of Al atoms in Cu.

Annealing temperatures were selected based on DSC measurements, which showed the presence of a wide peak in the temperature range 150–450 °C. An X-ray phase analysis of the composite immediately after deformation, along with Al and Cu, revealed 0.5% of the Al₂Cu phase. As expected, the formation of the maximum fraction of intermetallic compounds occurred after annealing at a maximum of the DSC peak temperature—450 °C (Fig. 4). The total proportion of intermetallic phases in the composite after annealing at 450° for 30 min was 49.5%. In this case, the Al₂Cu, AlCu, Al₄Cu₉ intermetallics were detected in the composite, which, on the whole, agrees with the observations of other authors studying Al and Cu bonded with different deformation methods [3,31,32].

Figure 5 shows the microstructure and EDS data in different parts of the sample after annealing at 450 °C for 30 min. As can be seen in the SEM images, in addition to dark areas corresponding to Al and white areas corresponding to Cu, layers of dark gray, gray and light gray color with clear boundaries are revealed. Energy-dispersive analysis showed that the dark and white areas consist of Al and Cu, respectively, and when passing from dark gray to gray and light gray layers, the ratio of Al and Cu changes stepwise and the EDS for individual points showed that the observed gray zones correspond to Al₂Cu compounds, AlCu, Al₄Cu₉, with Al₄Cu₉ layers adjacent to Cu layers, and Al₂Cu layers to Al. The maximum proportion of intermetallic phases is observed near the edge of the disk sample, which is associated with maximum shear deformation at the edge and, consequently, with the formation of a highly defective ultrafine-grained structure, providing the best conditions for mechanical alloying of components.

3.3 Microhardness evaluation

The microhardness (HV) measurements along the radius line of the sample from the center to the edge of the composite are shown in Fig. 6. The intervals of HV values corresponding to the intermetallic phases Al₂Cu, Al₄Cu₉, AlCu, Al₃Cu₄ are highlighted and shaded [17], obtained by statistically reliable measurements on the longitudinal section of the sample on large grains of intermetallic phases Al₂Cu, Al₄Cu₉, AlCu, Al₃Cu₄ identified by EDS analysis [32]. It is seen that before annealing, the microhardness generally increases with distance from the center and reaches maximum values near the sample periphery, which is apparently associated

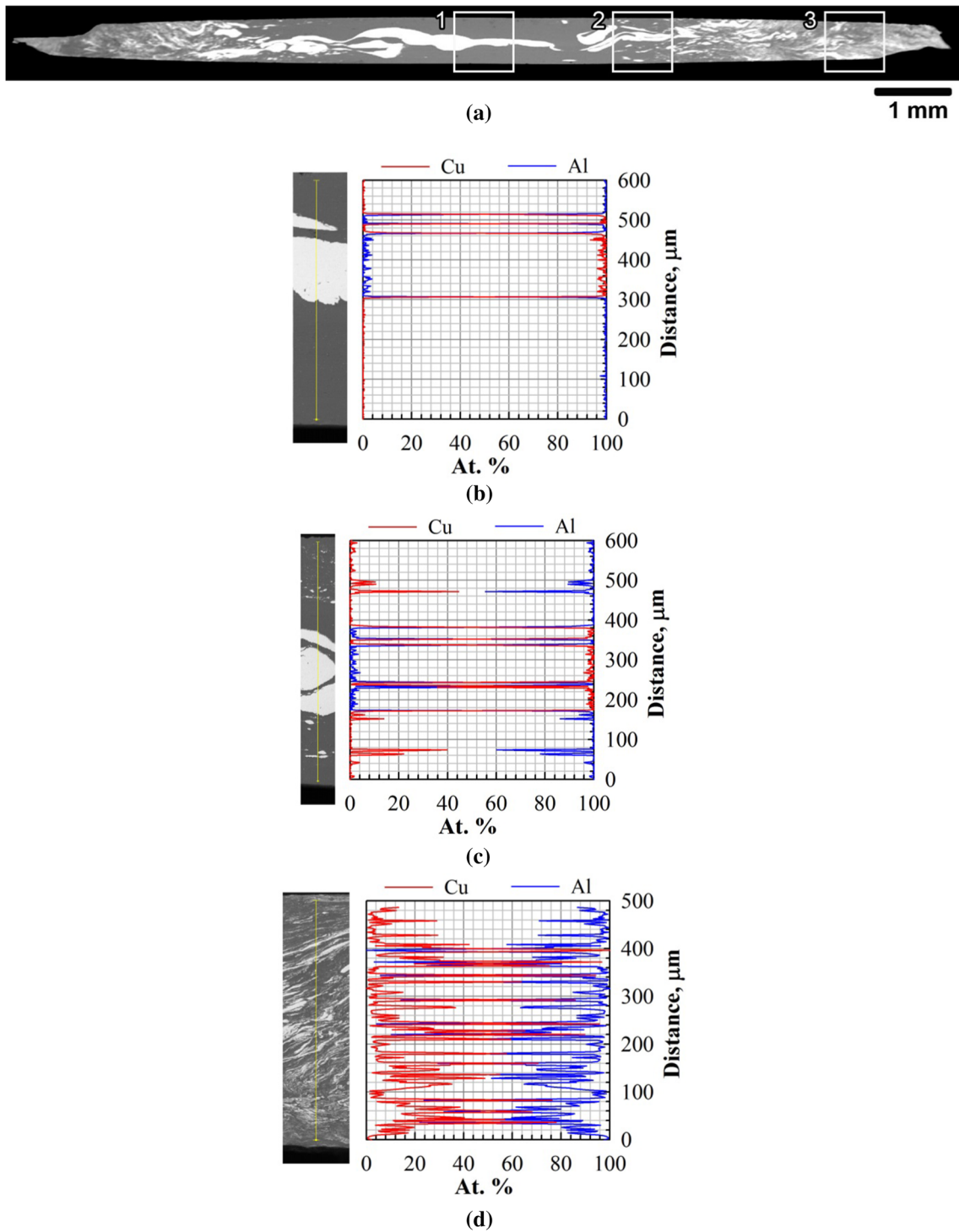


Fig. 2 BSE image of the Al–Cu–Al sample in the as-processed state at a small magnification (a) microstructure details in the center (1), at mid-radius (2), at the peripheral area (3). Elemental distribution along the line in the form of a graph of relative intensities with relation to the scanning distance for Cu and Al, in the center (b), at mid-radius (c) and in the peripheral area (d)

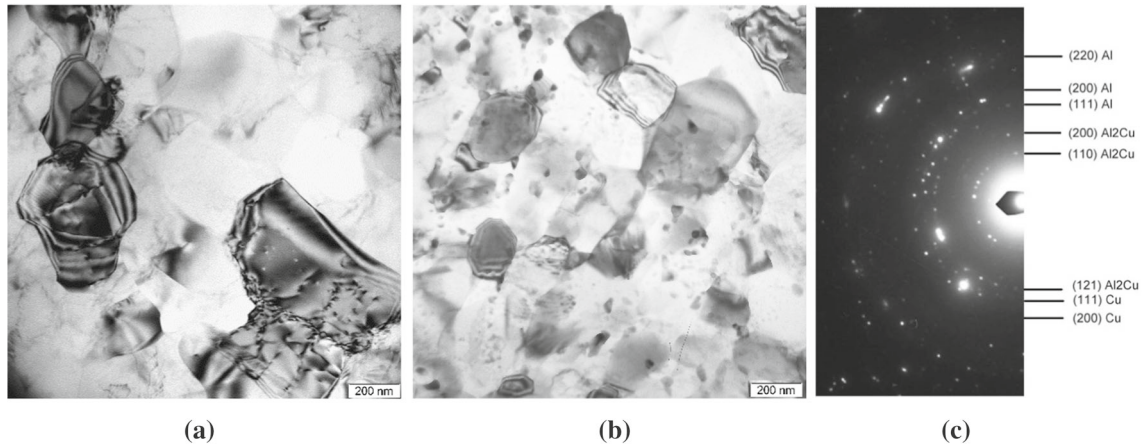


Fig. 3 Microstructure (TEM) of an Al–Cu–Al composite: **a** at mid-radius, **b** in the peripheral area, **c** electron diffraction pattern (SAED pattern) from the peripheral area

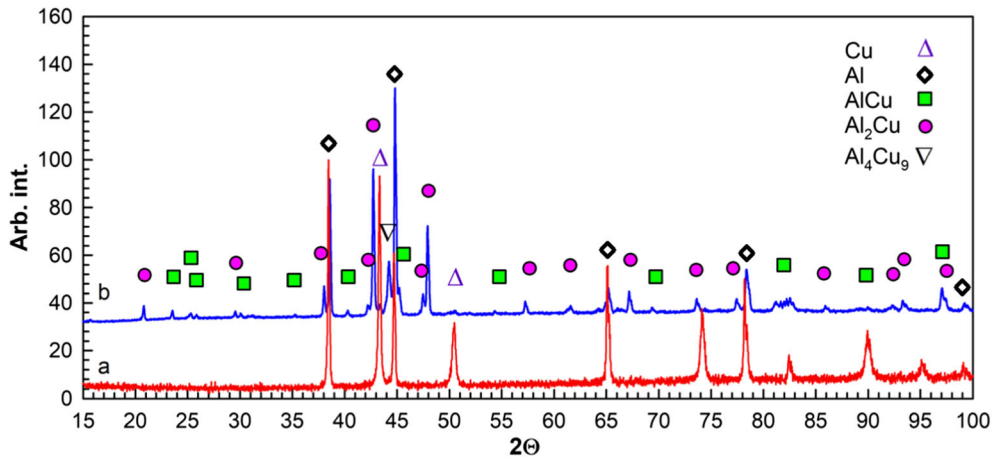


Fig. 4 XRD of the Al–Cu–Al samples before (red line) and after annealing at 450° for 15 min (blue line) (color figure online)

with a greater degree of strain and greater hardening at the sample edge. However, microhardness values vary nonmonotonically. In the center, where the fraction of interphase boundaries is small, the microhardness values do not differ much. With increasing distance from the center, the spread in HV values increases, which is obviously associated with different microhardness of the components, inhomogeneous sizes of structural components and hardening at the Al/Cu interfaces.

A certain decrease in the HV of the aluminum matrix, which is especially clearly seen in the center of the sample, is obviously the consequence of annealing-driven recrystallization. The appearance of points with high HV values at the distance of 2 mm or more from the center is due to the formation of intermetallic phases during annealing. A comparison of the obtained microhardness values with measurements on the identified intermetallic phases indicates that the main phase after annealing is Al₂Cu. Overall, the structure obtained in the composite can be characterized as heterogeneous, consisting of a ductile aluminum matrix and hard inclusions of intermetallic compounds with a gradient increase in microhardness from the center to the edge of the sample.

In order to estimate the distribution of intermetallic phases in the composite after annealing and analyze their contribution in the structure of the sample, the analysis of microhardness values with subsequent chemical analysis of different phases was performed. Figure 7 shows the measurement scheme on the area located in the middle sample radius where microhardness prints are sequentially numbered and the obtained values are provided in Table 1.

Analysis of microhardness measurement of composite components reveals that most of intermetallic phases are formed along the initial Al–Cu boundaries formed during the HPT process. The copper enriched phase

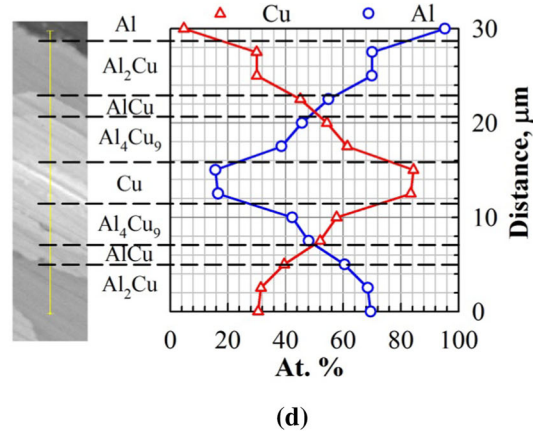
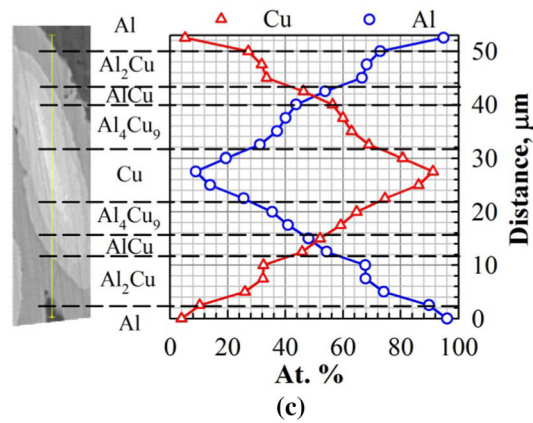
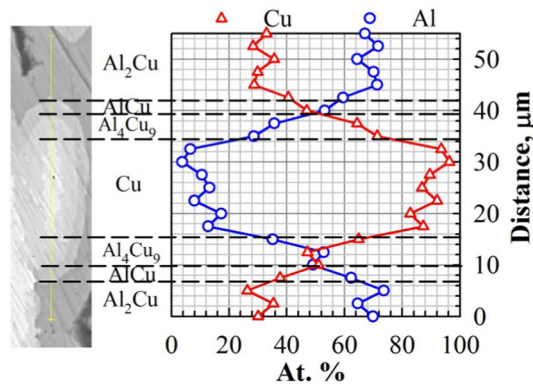
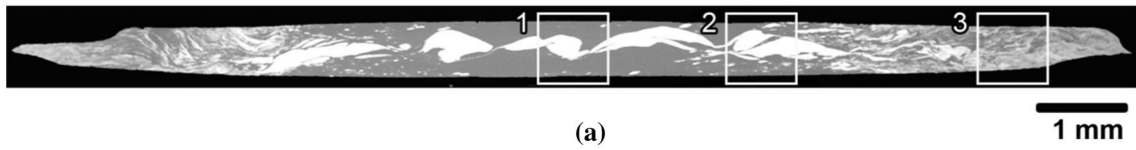


Fig. 5 BSE image of the Al–Cu–Al sample after annealing at 450 °C for 30 min at small magnification (a) the area in white square represents the typical microstructure type in the center (1), at mid-radius (2), at the peripheral area (3). Elemental distribution along the line in the form of a graph of relative intensities with relation to the scanning distance for Cu and Al, in the center (b), at mid-radius (c) and in the peripheral area (d)

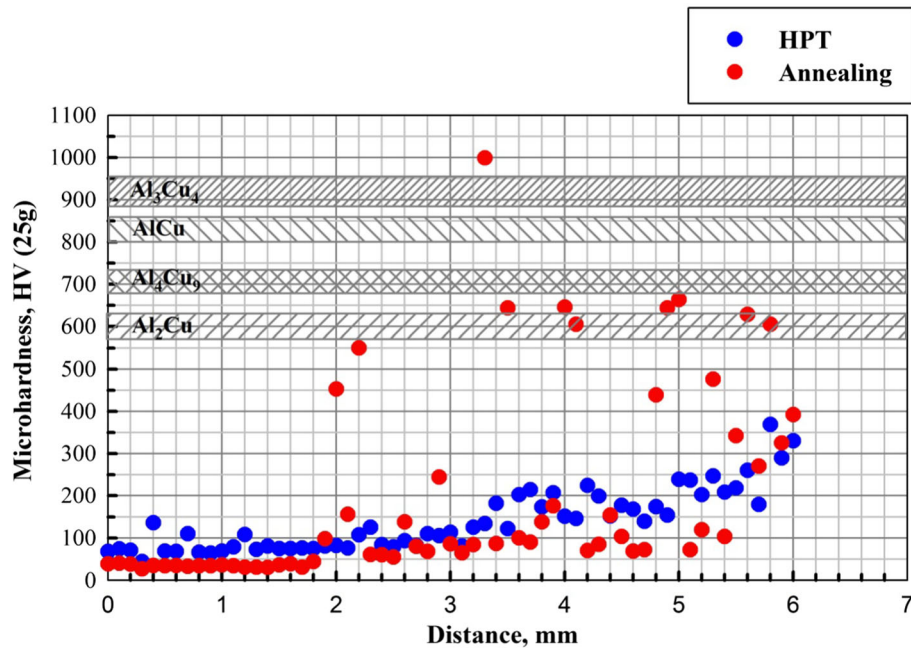


Fig. 6 Microhardness of Al–Cu–Al composite in as-processed state and after annealing at 450 °C during 30 min and comparison with microhardness values for Al_2Cu , Al_4Cu_9 , AlCu , Al_3Cu_4 [32]

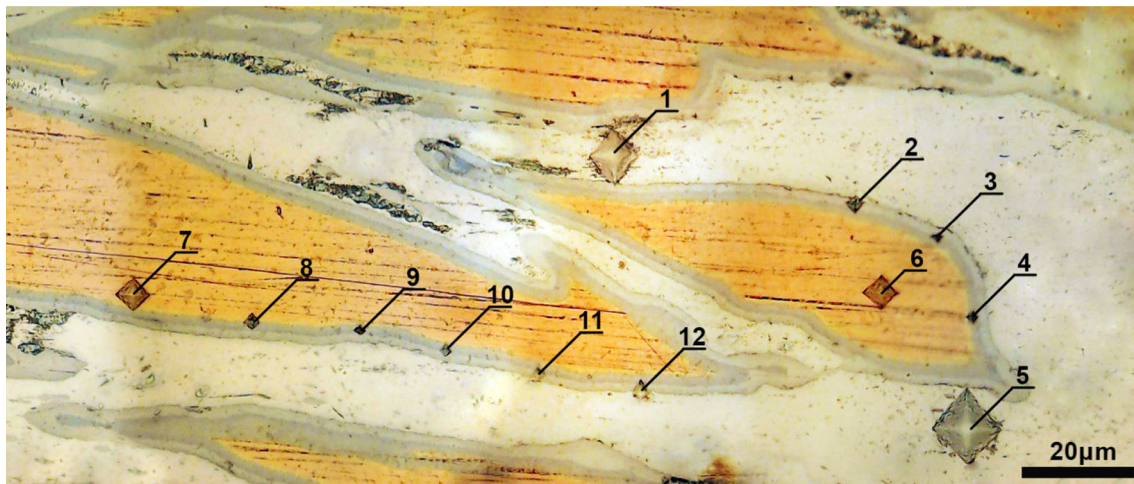


Fig. 7 Scheme of cross section microhardness measurement of Al–Cu–Al composites after annealing at 450 °C during 30 min. Reddish color corresponds to Cu phase, light grey goes for Al, and darker shades of gray correspond to annealing-induced intermetallic phases. The values of microhardness and chemical composition of numbered prints are given in Table 1 (color figure online)

Al_4Cu_9 layer located near the Cu phase has the highest microhardness values among all measured components. Another intermetallic phase Al_2Cu is adjacent to the pure Al part. Particles of the equiatomic composition phase AlCu were discovered at the interface between the two previously mentioned phases. The problem with the mismatch of microhardness values for points 4 and 12 in Table 1 is the results of the features of the EDS analysis. Results of phase identification in EDS depend on the interphase boundary tilt angle and the analyzed volume of the material that cannot be smaller than some critical value. It should be mentioned that the minimal critical volume required for EDS analysis is in some cases larger than the microhardness print size. According

Table 1 Microhardness values and local chemical composition of prints shown in Fig. 7

Measurement no.	Al, wt%	Cu, wt%	Phase	HV
1	97	3	Al	48
2	70	30	Al ₂ Cu	337
3	64	36	Al ₂ Cu	578
4	N/D	N/D	N/D	541
5	98	2	Al	26
6	0	100	Cu	82
7	0	100	Cu	93
8	18	82	Cu	421
9	26	74	Al ₄ Cu ₉	778
10	32	68	Al ₄ Cu ₉	865
11	50	50	AlCu	655
12	N/D	N/D	N/D	381

to these reasons, it was concluded that the precise measurement of the local chemical composition in points 4 and 12 was not possible, which is reflected in Table 1 accordingly as not definable (N/D).

An analysis of the evolution of the chemical composition of the phases upon distancing from the pure metal indicates that their formation is highly likely the result of annealing-induced lattice diffusion. However, this statement can be confirmed after analyzing the kinetics of phase formation during annealing.

3.4 Growth kinetics of intermetallic phases

To analyze the kinetics of phase transformations, annealing was carried out at low temperatures: 150, 170, 190 and 210 °C. The phase transformation rate was estimated according to X-ray phase analysis during isothermal annealing after selected time intervals. Figure 8 shows the evolution of the volume fractions of the Al₂Cu, AlCu, and Al₄Cu₉ phases as a function of square root of the annealing time for isothermal annealing at temperatures of 150, 170, 190 and 210 °C. The fraction of intermetallic phases grows upon the annealing time increase for all analyzed temperatures, but the growth turned out to be nonmonotonic. It is clearly seen that in all the graphs, two growth periods can be distinguished—in the first period, the most intensive growth of the volume fraction of all phases occurs followed by stabilization, and then, in the second stage, the volume fraction of phases slowly increases.

Such a double step character of the curves indicates that the process of growth of intermetallic phases in the Al–Cu–Al composite obtained by severe deformation develops in two stages. The first one corresponds to nucleation of Al₂Cu intermetallics at the boundaries of the Al/Cu layer joint at room temperature. Supersaturation of Al and Cu solid solutions and high density of defects can promote the formation of Al₂Cu phase even before the annealing. The second stage takes place during annealing when the AlCu phase is formed at the boundaries of the Al₂Cu and Cu components, followed by Al₄Cu₉ phase nucleation and growth as shown in Fig. 5. Such a sequence of intermetallics was also observed in [31]. The high defect density accumulated during deformation, specifically point defects [33], contributes significantly to mass transfer in crystals and promotes diffusion and formation of solid solutions at the Al/Cu boundaries, which in turn results in the formation of a small fraction (about 0.5%, see Fig. 8) of the Al₂Cu phase already at room temperature and the growth of all three intermetallic phases at the initial step of annealing.

At the first stage, the growth of intermetallic phases is limited by solid solutions depletion. Depletion of the adjacent layers and annealing-induced decrease in defects density result in temporary stabilization of intermetallic compounds fraction. Another reason for growth retardation is the fact that the newly formed layers of Al₂Cu, AlCu, Al₄Cu₉ compounds become an obstacle to the diffusion of Cu and Al atoms from one layer to another. Therefore, in the second stage, the growth rate is significantly reduced. The first stage of growth turned out to be much longer at lower annealing temperatures of 150 and 170 °C; here, the volume fraction of intermetallic phases increased sharply during the first 5 min. With an increase in temperature to 190 and 210 °C, depletion of the solid solution occurs faster and the steps on the curve shift to shorter times.

The relationship between the volume fraction of intermetallic compounds and the annealing time at a certain temperature can be described by the formula

$$V = V_0 + Kt^n,$$

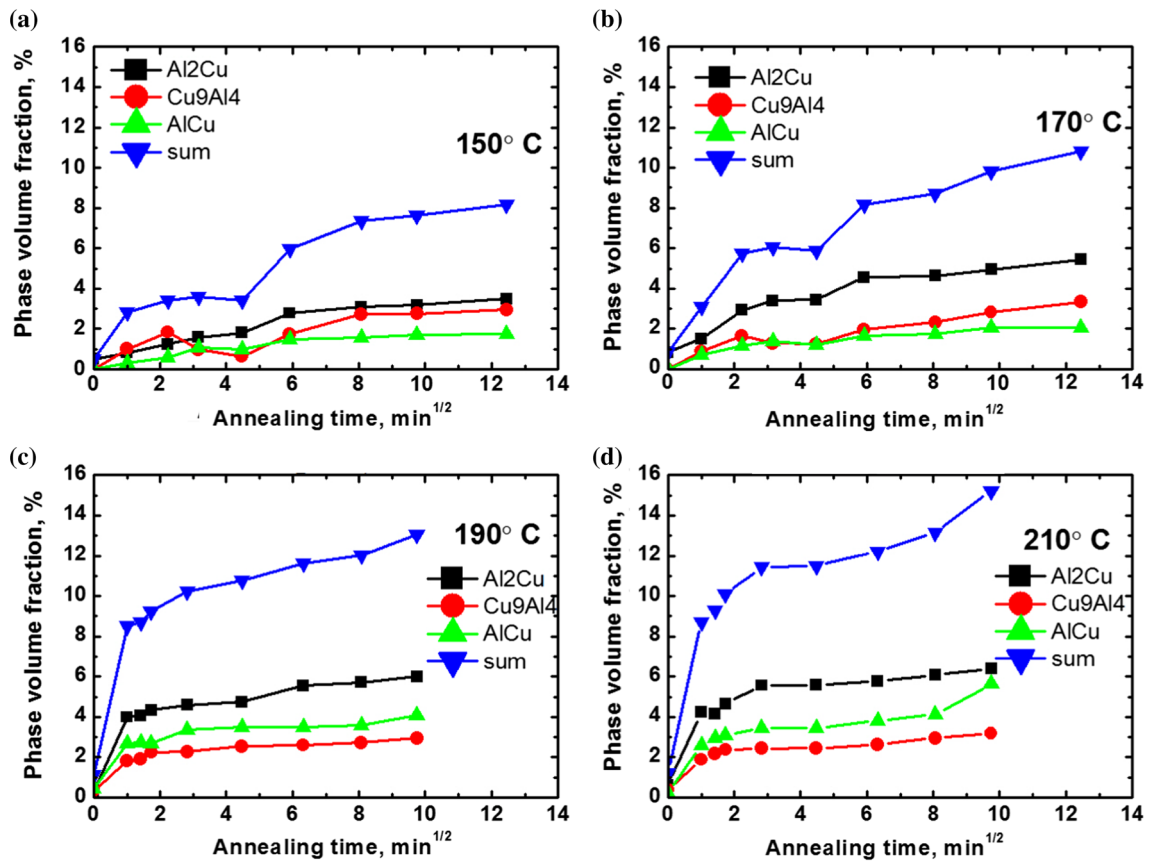


Fig. 8 The volume fraction of the Al_2Cu , AlCu and Al_4Cu_9 phases as a function of time during annealing at 150, 170, 190 and 210 °C

where V is the volume of the phase, V_0 is the initial volume, K is the temperature-dependent growth rate constant, t is the annealing time, and n is the exponent. If the phase growth process is controlled by volume diffusion, n is equal to $1/2$, and when controlled by grain-boundary diffusion, n is $1/3$ [34]. The experimental data for all analyzed annealing temperatures showed better agreement with the approximation of $t^{1/2}$ (see Fig. 8), which indicates that the growth of intermetallic compounds AlCu and Al_2Cu in the composite obtained by the SPD of the initial plates of pure components is controlled by volume diffusion. Similar dependences were obtained by other authors for the formation of Al_2Cu intermetallic compounds on deposited [14] and electrodeposited Al–Cu layered samples [35]. One should also mention that for the Al_4Cu_9 phase the dependence of the phase volume on the annealing time was nonmonotonous. Partial dissolution of this phase was observed at 150 °C and 170 °C in the annealing time interval 5–15 min. This fact did not allow us to perform the activation energy estimation for this case. To calculate the activation energy at the initial stage of growth, we used measurements of the volume fraction of the Al_2Cu and AlCu phases at all annealing temperatures in the time interval of 1–20 min (Fig. 8).

The activation energy of phase growth can be obtained from the Arrhenius equation for the temperature dependence of the growth rate s :

$$s = s_0 \times e^{(-E_a/RT)},$$

where K_0 is the pre-exponential factor, E_a is the activation energy, R is the universal gas constant, and T is the absolute temperature (K). Representing this equation in a logarithmic form, we obtain

$$\ln s = \ln s_0 - E_a/RT,$$

which allows us to calculate the activation energy of intermetallic phases from the plot $\ln(s) = f(1/T)$ (Fig. 9).

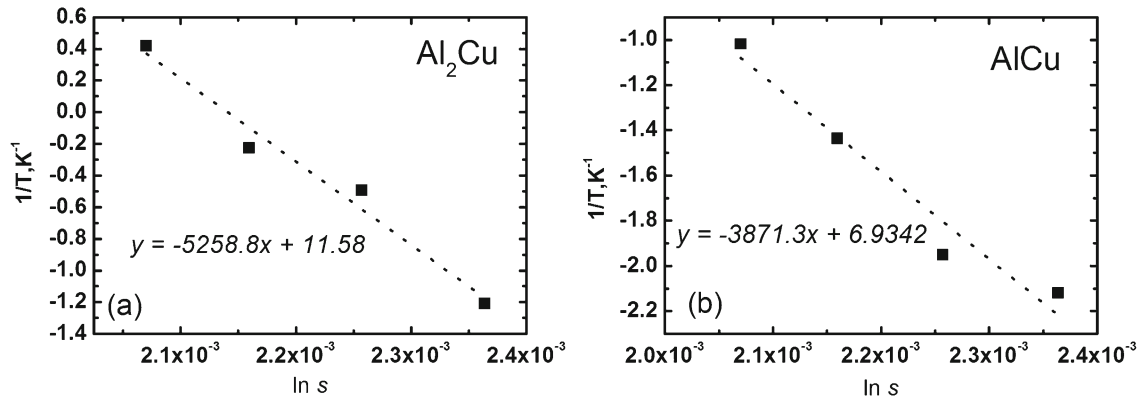


Fig. 9 Arrhenius plot for determination of the activation energy for growth of Al₂Cu (a) and AlCu (b)

Thus, for the Al₂Cu phase calculations were performed as follows:

$$E_a = R \times \text{tg}\alpha;$$

$$\text{tg}\alpha = 5528,8; \quad R = 8314 \text{ J/(K mol)},$$

$$E_a = 45966 \text{ J/mol} = 0.4764041 \text{ eV}.$$

Similar calculations for the activation energy of AlCu gave values:

$$\text{tg}\alpha = 3871,3,$$

$$E_a = 32170.5 \text{ J/mol} = 0.33 \text{ eV}.$$

According to these calculations, the growth of intermetallic compounds in the composite upon annealing occurs due to the predominant diffusion of Cu atoms in Al. The experimental activation energy obtained in this work turned out to be significantly lower than the activation energy of bulk diffusion of Cu in polycrystalline Al, which is 1.4 eV [36]. In [32], in the Cu/Al composite obtained by cold rolling, the activation energies for CuAl₂ were 97.5 kJ/mol (1.01 eV) and for Al₄Cu₉ 107.85 kJ/mol (1.12 eV), and in the electrodeposit layered the Cu/Al composite (electroplated Cu/Al laminar composites), the activation energy for Al₂Cu was 25.47 kJ/mol (0.26 eV) and 34.16 kJ/mol (0.35 eV) for Al₄Cu₉ [35], which the authors attributed to pores and defects in the crystal structure. Different values of the activation energy of the intermetallic compounds growth are associated, obviously, with differences of their processing route. The activation energy values closest to those calculated by us were obtained in [37]. The activation energy obtained in an Al—3 wt% Cu alloy subjected to HPT for Al₂Cu was 47.9 kJ/mol (0.49 eV) and 50.2 kJ/mol (0.52 eV) when calculated by models for bulk and grain boundary diffusion, respectively [38].

4 Phase transformation-induced evolution of mechanical properties

Mechanical tests of the metal-matrix composite revealed the average value of the ultimate tensile strength to reach 485 MPa. This exceeds by several times the ultimate tensile strength of the initial components obtained under same conditions (~ 80 MPa and ~ 190 MPa for pure Al and Cu, respectively [39]). Thus, the ultimate strength of heterostructure type Al—Cu—Al composite is much higher than that predicted by the mixture rule [37] that can be explained by the so-called hetero-deformation-induced back stress [40] being caused by the presence of high density of geometrically necessary dislocation in the material subjected to severe strain. This type of dislocations is emerged in the soft phase (Al) in the vicinity of the phase boundary. The formed pileups can increase the soft phase strength up to values comparable to that of the hard phase. The overall hardness of the composite in this case can be higher than the mechanical characteristics of both composite components. The ultimate condition for this scenario is the presence of high pressure and shear strain or other mechanism providing the tight bonding of components.

The presence of high defects density and internal strains after high-pressure torsion can promote the bulk diffusion of components resulting in formation of intermetallic phases precipitates that in turn lead to drop of dislocation density and formation of weak bonds in the areas of phase boundaries. Such phase transformations

result in degradation of back stress and an overall decrease in the matrix microhardness and ultimate strength with a corresponding change of the major deformation mechanisms realized during loading [39].

Another factor leading to the strength decrease is the layered structure of intermetallic phases (see Fig. 7) accompanied by the poor joint quality that can serve as the hot spot for crack initiation. However, this hypothesis requires further investigations before being ultimately claimed.

5 Conclusions

In summary, in the present work, we have performed an extended analysis of microstructure, mechanical properties and phase composition in an Al–Cu–Al composite obtained by HPT in as-deformed and annealed states.

- The microstructure after HPT has a heterogeneous submicron grained multilayered type with a gradual decrease in size from the center to the edge. A small amount of Al_2Cu precipitations in the as-deformed state was revealed both by TEM observations and XRD phase analysis.
- Three intermetallic sublayers Al_2Cu , AlCu and Al_4Cu_9 with an increased microhardness value were gradually formed and developed in the composite during annealing. The volume fraction of these intermetallic phases increased consistently with increasing annealing time and temperature.
- The growth kinetics of intermetallic compounds was analyzed and found to follow the patterns of a diffusion-limited process. The activation energy of intermetallic phase growth was estimated and revealed to be much lower than the bulk diffusion value. The difference may result from extremely high concentration of defects, e.g., vacancies, pores and grain boundaries in the structure of composite after HPT that drastically promotes the diffusion of Cu atoms accelerating the formation and growth of the Al_2Cu , AlCu and Al_4Cu_9 intermetallics in the studied composite.
- It was shown that maximal microhardness values are revealed in the Al_9Cu_4 phase that undergoes a partial dissolution during long-term annealing. This fact allows to propose that thermomechanical treatment regime associated with improved mechanical properties should be performed in limited time at moderate temperature in order to avoid the strengthening phase dissolution.

Summarizing the above-mentioned findings with analysis of mechanical properties [39], one can conclude that maximal level of tensile strain corresponds to the HPT-induced mixture of initial components with 0.5% of the Al_2Cu phase (according to XRD data, see Fig. 4). However, this structural state is not stable even at room temperature. After the annealing at 450 °C, nucleation and growth of intermetallic precipitates result in degradation of both strength and ductility. Thus, for obtaining the structure with both thermal stability and fair mechanical characteristics, knowledge of kinetics of corresponding to intermetallic phases nucleation and growth can be an essential factor allowing to control the dynamics of structure evolution upon annealing.

The Arrhenius plot given in Fig. 9 allows to select the regimes corresponding to the maximal intensity of intermetallic phase nucleation while avoiding their growth ($T = 150\text{--}170\text{ }^\circ\text{C}$, $t < 2\text{--}3\text{ min}$). This type of structure is expected to be characterized by enhanced thermal stability together with elevated mechanical characteristics.

Based on the performed research, one can conclude that the main factors governing the mechanical characteristics of Al–Cu–Al composites are initial (i) structure (in)homogeneity, (ii) presence of hetero-deformation-induced back stress and (iii) annealing-induced formation of intermetallic phases. This work contributes to the analysis of the mentioned factors providing the basic insights for thermal treatment regimes aimed at creating maximal density of intermetallic precipitates of minimal size that, in turn, increase the role of precipitation strengthening in the complex of mechanical properties in the Al–Cu–Al hybrid composite.

Acknowledgements The present work was accomplished according to the state assignment of IMSP RAS and supported by the Russian Science Foundation (Grant No. 18-12-00440).

Compliance with ethical standards

Conflict of interest The authors declare that they have no known competing financial interests or personal relationships that could have appeared to influence the work reported in this paper.

References

1. Han, J.-K., Han, D.K., Liang, G.Y., Jang, J.-I., Langdon, T.G., Kawasaki, M.: Direct bonding of aluminum–copper metals Through high-pressure torsion processing. *Adv. Eng. Mater.* **20**, 1800642 (2018). <https://doi.org/10.1002/adem.201800642>
2. Kawasaki, M., Han, J.-K., Lee, D.-H., Jang, J., Langdon, T.G.: Fabrication of nanocomposites through diffusion bonding under high-pressure torsion. *J. Mater. Res.* **33**, 2700–2710 (2018). <https://doi.org/10.1557/jmr.2018.205>
3. Oh-ishi, K., Edalati, K., Kim, H.S., Hono, K., Horita, Z.: High-pressure torsion for enhanced atomic diffusion and promoting solid-state reactions in the aluminum–copper system. *Acta Mater.* **61**, 3482–3489 (2013). <https://doi.org/10.1016/j.actamat.2013.02.042>
4. Mishler, M., Ouvarov-Bancalero, V., Chae, S.H., Nguyen, L., Kim, C.-U.: Intermetallic compound growth and stress development in Al–Cu diffusion couple. *J. Elect. Mater.* **47**, 855–865 (2018). <https://doi.org/10.1007/s11664-017-5877-y>
5. Rahmatatabadi, D., Tayyebi, M., Hashemi, R., Faraji, G.: Microstructure and mechanical properties of Al/Cu/Mg laminated composite sheets produced by the ARB proces. *Int. J. Miner. Metall. Mater.* **25**, 564–572 (2018). <https://doi.org/10.1007/s12613-018-1603-x>
6. Aikin, R.M.: The mechanical properties of in-situ composites. *JOM* **49**, 35–39 (1997). <https://doi.org/10.1007/BF02914400>
7. Bandyopadhyay, N.R., Ghosh, S., Basumallick, A.: New generation metal matrix composites. *Mater. Manuf. Process.* **22**, 679–682 (2007). <https://doi.org/10.1080/10426910701384872>
8. Tjong, S.: Microstructural and mechanical characteristics of in situ metal matrix composites. *Mater. Sci. Eng.: R: Rep.* **29**, 49–113 (2000). [https://doi.org/10.1016/S0927-796X\(00\)00024-3](https://doi.org/10.1016/S0927-796X(00)00024-3)
9. Das, S., Das, S., Das, K.: Abrasive wear of zircon sand and alumina reinforced Al–4.5 wt% Cu alloy matrix composites—a comparative study. *Compos. Sci. Technol.* **67**, 746–751 (2007). <https://doi.org/10.1016/j.compscitech.2006.05.001>
10. Surappa, M.K.: Aluminium matrix composites: challenges and opportunities. *Sadhana* **28**, 319–334 (2003). <https://doi.org/10.1007/BF02717141>
11. Bodunrin, M.O., Alaneme, K.K., Chown, L.H.: Aluminium matrix hybrid composites: a review of reinforcement philosophies; mechanical, corrosion and tribological characteristics. *J. Mater. Res. Technol.* **4**, 434–445 (2015). <https://doi.org/10.1016/j.jmrt.2015.05.003>
12. Mohapatra, S., Chaubey, A.K., Mishra, D.K., Singh, S.K.: Fabrication of Al–TiC composites by hot consolidation technique: its microstructure and mechanical properties. *J. Mater. Res. Technol.* **5**, 117–122 (2016). <https://doi.org/10.1016/j.jmrt.2015.07.001>
13. Bihari, B., Singh, A.K.: An overview on different processing parameters in particulate reinforced metal matrix composite fabricated by stir casting process. *Int. J. Eng. Res. Appl.* **7**, 42–48 (2017). <https://doi.org/10.9790/9622-0701034248>
14. Sheibani, S.: In situ fabrication of Al–TiC metal matrix composites by reactive slag process. *Mater. Des.* **28**, 2373–2378 (2007). <https://doi.org/10.1016/j.matdes.2006.08.004>
15. Karantzalis, A.E., Wyatt, S., Kennedy, A.R.: The mechanical properties of Al–TiC metal matrix composites fabricated by a flux-casting technique. *Mater. Sci. Eng.: A* **237**, 200–206 (1997). [https://doi.org/10.1016/S0921-5093\(97\)00290-6](https://doi.org/10.1016/S0921-5093(97)00290-6)
16. Shockley, J.M., Strauss, H.W., Chromik, R.R., Brodusch, N., Gauvin, R., Irissou, E., Legoux, J.-G.: In situ tribometry of cold-sprayed Al–Al₂O₃ composite coatings. *Surf. Coat. Technol.* **215**, 350–356 (2013). <https://doi.org/10.1016/j.surfcoat.2012.04.099>
17. Das, B., Roy, S., Rai, R.N., Saha, S.C.: Development of an in-situ synthesized multi-component reinforced Al–4.5% Cu–TiC metal matrix composite by FAS technique—optimization of process parameters. *Eng. Sci. Technol., Int. J.* **19**, 279–291 (2016). <https://doi.org/10.1016/j.jestch.2015.08.002>
18. Zhang, Z., Topping, T., Li, Y., Vogt, R., Zhou, Y., Haines, C., Paras, J., Kapoor, D., Schoenung, J.M., Lavernia, E.J.: Mechanical behavior of ultrafine-grained Al composites reinforced with B4C nanoparticles. *Scr. Mater.* **65**, 652–655 (2011). <https://doi.org/10.1016/j.scriptamat.2011.06.037>
19. Kawasaki, M., Jang, J.: Micro-mechanical response of an Al–Mg hybrid system synthesized by high-pressure torsion. *Materials* **10**, 596 (2017). <https://doi.org/10.3390/ma10060596>
20. Korznikova, G., Kabirov, R., Nazarov, K., Khisamov, R., Shayakhmetov, R., Korznikova, E., Khalikova, G., Mulyukov, R.: Influence of constrained high-pressure torsion on microstructure and mechanical properties of an aluminum-based metal matrix composite. *JOM* (2020). <https://doi.org/10.1007/s11837-020-04152-1>
21. Zhang, X., Yu, Y., Liu, B., Zhao, Y., Ren, J., Yan, Y., Cao, R., Chen, J.: In-situ investigation of deformation behavior and fracture mechanism of laminated Al/Ti composites fabricated by hot rolling. *J. Alloys Compd.* **783**, 55–65 (2019). <https://doi.org/10.1016/j.jallcom.2018.12.272>
22. Hernández-Escobar, D., Rahman, Z.U., Yilmazer, H., Kawasaki, M., Boehlert, C.J.: Microstructural evolution and intermetallic formation in Zn–Mg hybrids processed by high-pressure torsion. *Philos. Maga.* **99**, 557–584 (2019). <https://doi.org/10.1080/14786435.2018.1546962>
23. Ru, Y., Yu, K.Y., Guo, F., Ren, Y., Cui, L.: Temperature-dependent plastic deformation mechanisms of a Cu/steel transforming nanolamellar composite. *Mater. Sci. Eng.: A* **734**, 77–84 (2018). <https://doi.org/10.1016/j.msea.2018.07.090>
24. Rogachev, S.O., Nikulin, S.A., Khatkevich, V.M., Sundeev, R.V., Kozlov, D.A.: High-pressure torsion deformation process of bronze/niobium composite. *Trans. Nonferrous Metals Soc. China* **29**, 1689–1695 (2019). [https://doi.org/10.1016/S1003-6326\(19\)65075-2](https://doi.org/10.1016/S1003-6326(19)65075-2)
25. Korznikova, G., Czeppe, T., Khalikova, G., Gunderov, D., Korznikova, E., Litynska-Dobrzynska, L., Szlezzynger, M.: Microstructure and mechanical properties of Cu–graphene composites produced by two high pressure torsion procedures. *Mater. Charact.* **161**, 110122 (2020). <https://doi.org/10.1016/j.matchar.2020.110122>
26. Liu, X.J., Ohnuma, I., Kainuma, R., Ishida, K.: Phase equilibria in the Cu–Al binary system. *J. Alloys Compd.* **264**, 201–208 (1998). [https://doi.org/10.1016/S0925-8388\(97\)00235-1](https://doi.org/10.1016/S0925-8388(97)00235-1)
27. Zhilyaev, A., Langdon, T.: Using high-pressure torsion for metal processing: fundamentals and applications. *Prog. Mater. Sci.* **53**, 893–979 (2008). <https://doi.org/10.1016/j.pmatsci.2008.03.002>
28. Mulyukov, K.Y., Korznikova, G.F., Nikitin, S.A.: Magnetization of nanocrystalline dysprosium: annealing effects. *J. Appl. Phys.* **79**, 8584–8587 (1996). <https://doi.org/10.1063/1.362478>

29. Sapanathan, T., Khoddam, S., Zahiri, S.H., Zarei-Hanzaki, A., Ibrahim, R.: Hybrid metallic composite materials fabricated by sheathed powder compaction. *J. Mater. Sci.* **51**, 3118–3124 (2016). <https://doi.org/10.1007/s10853-015-9621-9>
30. Korznikova, G.F., Nazarov, K.S., Khisamov, R.K., Sergeev, S.N., Shayachmetov, R.U., Khalikova, G.R., Baimova, J.A., Glezer, A.M., Mulyukov, R.R.: Intermetallic growth kinetics and microstructure evolution in Al–Cu–Al metal-matrix composite processed by high pressure torsion. *Mater. Lett.* **253**, 412–415 (2019). <https://doi.org/10.1016/j.matlet.2019.07.124>
31. Hentzell, H.T.G., Thompson, R.D., Tu, K.N.: Interdiffusion in copper-aluminum thin film bilayers. I. Structure and kinetics of sequential compound formation. *J. Appl. Phys.* **54**, 6923–6928 (1983). <https://doi.org/10.1063/1.331999>
32. Chen, C.-Y., Hwang, W.-S.: Effect of annealing on the interfacial structure of aluminum–copper joints. *Mater. Trans.* **48**, 1938–1947 (2007). <https://doi.org/10.2320/matertrans.MER2006371>
33. Korznikova, E.A., Mironov, S.Y., Korznikov, A.V., Zhilyaev, A.P., Langdon, T.G.: Microstructural evolution and electro-resistivity in HPT nickel. *Mater. Sci. Eng.: A* **556**, 437–445 (2012). <https://doi.org/10.1016/j.msea.2012.07.010>
34. Cahn, R.W., Haasen, P. (eds.): *Physical Metallurgy*. North-Holland, Amsterdam, New York (1996)
35. Zhang, J., Wang, B., Chen, G., Wang, R., Miao, C., Zheng, Z., Tang, W.: Formation and growth of Cu–Al IMCs and their effect on electrical property of electroplated Cu/Al laminar composites. *Trans. Nonferrous Metals Soc. China* **26**, 3283–3291 (2016). [https://doi.org/10.1016/S1003-6326\(16\)64462-X](https://doi.org/10.1016/S1003-6326(16)64462-X)
36. Peterson, N.L., Rothman, S.J.: Impurity diffusion in aluminum. *Phys. Rev. B* **1**, 3264–3273 (1970). <https://doi.org/10.1103/PhysRevB.1.3264>
37. Ma, X.L., Huang, C.X., Xu, W.Z., Zhou, H., Wu, X.L., Zhu, Y.T.: Strain hardening and ductility in a coarse-grain/nanostructure laminate material. *Scr. Mater.* **103**, 57–60 (2015). <https://doi.org/10.1016/j.scriptamat.2015.03.006>
38. Rashkova, B., Faller, M., Pippan, R., Dehm, G.: Growth mechanism of Al₂Cu precipitates during in situ TEM heating of a HPT deformed Al–3 wt% Cu alloy. *J. Alloys Compd.* **600**, 43–50 (2014). <https://doi.org/10.1016/j.jallcom.2014.02.090>
39. Kabirov, R.R., Nazarov, K.S., Korznikova, G.F., Khisamov, R.K., Sergeyev, S.N., Nagimov, M.I., Mulyukov, R.R.: Mechanical properties of a metal-matrix composite based on copper and aluminum, obtained via shear deformation under pressure. *Bull. Russ. Acad. Sci.: Phys.* **83**, 1265–1269 (2019). <https://doi.org/10.3103/S1062873819100101>
40. Wu, X., Zhu, Y.: Heterogeneous materials: a new class of materials with unprecedented mechanical properties. *Mater. Res. Lett.* **5**, 527–532 (2017). <https://doi.org/10.1080/21663831.2017.1343208>

Publisher's Note Springer Nature remains neutral with regard to jurisdictional claims in published maps and institutional affiliations.